

12

AD A118383

AD

TECHNICAL REPORT ARBRL-TR-02412

TEMPERATURE PROFILE OF A STOICHIOMETRIC
CH₄/N₂O FLAME FROM LASER EXCITED
FLUORESCENCE MEASUREMENTS ON OH

William R. Anderson
Leon J. Decker
Anthony J. Kotlar

July 1982



US ARMY ARMAMENT RESEARCH AND DEVELOPMENT COMMAND
BALLISTIC RESEARCH LABORATORY
ABERDEEN PROVING GROUND, MARYLAND

DTIC FILE COPY

Approved for public release; distribution unlimited.

DTIC
ELECTE
AUG 19 1982

gc E

82 08 02 019

**Destroy this report when it is no longer needed.
Do NOT return it to the originator.**

Secondary distribution of this report is prohibited.

**Additional copies of this report may be obtained
from the National Technical Information Service,
U. S. Department of Commerce, Springfield, Virginia
22161.**

**The findings in this report are not to be construed as
an official Department of the Army position, unless
so designated by other authorized documents.**

*The use of trade names or manufacturers' names in this report
does not constitute endorsement of any commercial product.*

Unclassified

SECURITY CLASSIFICATION OF THIS PAGE(When Data Entered)

Abstract (Cont'd):

(20) to fluorescence spectra. A least squares curve-fitting technique which accounts for the various types of line broadening was developed and applied to two absorption lines in the (0,0) band. The resulting temperature profile is compared to that from fluorescence data reduced using Boltzmann plots. The more complicated curve-fitting approach was later applied to five lines in the spectrum using several combinations of fluorescence and absorption data. Results of all the aforementioned methods were compared to those from OH band reversal and N_2 vibrational Raman measurements at the same point in the post flame gases. Excellent agreement was achieved. The results are discussed with emphasis on both the fluorescence diagnostics and the characteristics of the CH_4/N_2O flame on the porous-plug burner.

UNCLASSIFIED

SECURITY CLASSIFICATION OF THIS PAGE(When Data Entered)

TABLE OF CONTENTS

LIST OF ILLUSTRATIONS.....5

I. INTRODUCTION.....7

II. EXPERIMENTAL.....9

III. RESULTS.....11

IV. DISCUSSION.....25

V. CONCLUSIONS.....31

REFERENCES.....32

APPENDIX A.....37

DISTRIBUTION LIST.....39

Accession For	
NTIS GRA&I	<input checked="" type="checkbox"/>
DTIC TAB	<input type="checkbox"/>
Unannounced	<input type="checkbox"/>
Justification _____	
By _____	
Distribution/	
Availability Codes	
Dist	Avail and/or Special
A	



LIST OF ILLUSTRATIONS

Figure	Page
1. Experimental Apparatus.....	10
2. OH (1,1) Band R-Branch Excitation Scan in CH ₄ /N ₂ O Flame.....	12
3. Horizontal Fluorescence Profile of the (1,1) R ₂ 9 Transition of OH in CH ₄ /N ₂ O Flame at 1 cm Height.....	14
4. Boltzmann Plot for a Typical Fluorescence Excitation Scan of the OH (1,1) Band in CH ₄ /N ₂ O Flame.....	16
5a. Vertical Temperature Profile in a Stoichiometric CH ₄ /N ₂ O Flame.....	18
5b. Comparison of Absorption and Fluorescence Results Showing the Rapid Climb in the First Millimeter and Temperature at 10 Millimeters.....	19
6. Burner Body Temperature at Several Points Below the Edge of the Burner Head.....	20
7. An Example of Data Used for Simultaneously Fitting Five Lines in the Absorption and Fluorescence Spectra of OH.....	22

I. INTRODUCTION

Use of laser based combustion diagnostics has increased significantly in the last ten years. Because of relatively high sensitivity, laser excited fluorescence (LEF) techniques are particularly well suited for monitoring trace species concentrations. A prerequisite for such concentration measurements is a knowledge of the temperature of the system. The LEF temperature measurement technique which has received the most attention is the method of rotational excitation scans¹⁻⁵. The method involves scanning of the laser excitation wavelength through several rotational transitions of the radical of interest. A detector, usually set up to view fluorescence in some other portion of the spectrum than the region of the excitation wavelength to avoid scattering, monitors fluorescence intensity as the laser is scanned. From such data, relative rotational populations in the ground electronic state and a corresponding temperature may be determined assuming a Boltzmann distribution.

Prior to this work, flame studies using the excitation scan technique have only involved pumping from the ground vibrational level of the OH $A^2\Sigma^+ + X^2\Pi$ system and only CH₄/air flames have been used. The first of such measurements were performed by Wang and Davis¹ who used a Bunsen burner. They excited transitions in the (1,0) vibrational band. Fluorescence from molecules collisionally transferred down to the $v' = 0$ vibrational level in the excited state was observed from the (0,0) band transition. Cattolica² also has studied OH fluorescence. In his studies a flat-flame burner was used and the fluorescence was both excited and monitored in the (0,0) band. In experiments by Bechtel³, a burner which produces a curved flame front was used. The (0,0) and (1,0) band transitions were pumped while fluorescence was monitored in the (0,0) band. Finally, in a somewhat different application, Crosley and coworkers⁴ measured excited state rotational distributions by looking at the resolved fluorescence obtained upon pumping several different

¹Wang, C.C. and Davis, Jr., L.I., "Ground State Population Distributions of OH Determined with a Tunable UV Laser," *Appl. Phys. Lett.*, Vol. 25, P. 34 (1974).

²Cattolica, R.J., "OH Rotational Temperature from Laser Induced Fluorescence," Sandia Report No. SAND 78-8614, 1978.

³Bechtel, J.H., "Temperature Measurements of the Hydroxyl Radical and Molecular Nitrogen in Premixed, Laminar Flames by Laser Techniques," *Appl. Opt.*, Vol. 18, p. 2100 (1979).

⁴(a) Smith, G.P., Crosley, D.R. and Davis, L.W., "Rotational Population Distributions in Laser-Excited OH in an Atmospheric Pressure Flame," Paper 3, Eastern Section Fall Meeting of the Combustion Institute, Atlanta, Georgia 1979. (b) Smith, G.P. and Crosley, D.R., "Quantitative Laser-Induced Fluorescence in OH," Eighteenth Symposium (International) on Combustion, Waterloo, Ontario, Canada, August 1980. (c) Smith, G.P. and Crosley, D.R., "Energy Transfer in $A^2\Sigma^+$ OH in Flames," Paper FA9, Thirty-Fifth Symposium on Molecular Spectroscopy, Columbus, Ohio, June 1980. (d) Crosley, D.R. and Smith, G.P., "Rotational Energy Transfer and LIF Temperature Measurements," submitted for publication.

⁵(a) Anderson, W.R., "Laser Excited Fluorescence Measurement of OH Rotational Temperatures in a CH₄/N₂O Flame," Paper 3, Eastern Section Fall Meeting of the Combustion Institute, Atlanta, Georgia, November 1979. (b) Anderson, W.R., Beyer, R.A., and Vanderhoff, J.A., "Laser Excited Fluorescence, Laser Raman and Band Reversal Temperature Measurements in CH₄/N₂O Flames," Paper FA1, Thirty-Fifth Symposium on Molecular Spectroscopy, Columbus, Ohio, June 1980.

rotational states of OH. A model for rotational redistribution was developed which predicts the effects of incomplete rotational equilibration in the excited A state on the measured temperatures.

In early work in this laboratory, the excitation scan technique was applied to the OH (0,0) band in Bunsen flames of CH₄/air and to flat flames of CH₄/N₂O on a sintered-porous-plug burner⁶. Strong absorption (> 30%) of the laser excitation beam was observed for many transitions in both types of flame even though the Bunsen flame was only about 1 cm wide. There is also undoubtedly strong self-absorption of the fluorescence by the flame gases. In spite of these problems, such scans often yielded straight-line Boltzmann plots, though the fits were poor and the temperatures much lower than expected (~ 1000K). Such effects were also observed by Cattolica². Somewhat less frequently in these early runs, (0,0) band scans yielded curved Boltzmann plots or plots with two straight line portions. Such effects almost certainly influenced the results of Wang and Davis¹ who attributed a plot with two straight-line portions to nonequilibrium distributions of OH in their Bunsen flame. Bechtel avoided these problems by using a burner-optical system design which afforded a very short path length within the flame³.

The present work concerns a different approach to avoid extensive depletion of the laser beam intensity and self-absorption problems (hereafter referred to collectively as absorption problems) even with relatively large flat flame burners. In this new approach⁵, fluorescence was excited in the (1,1) R-branch region of OH while emission from a spectrally dense region containing mostly (1,1) band P- and Q-branch lines was observed. The population in the $v'' = 1$ level, where v'' is the ground vibrational quantum number, is about an order of magnitude less than the $v'' = 0$ level for temperatures found in most flames with a corresponding drop in the amount of absorption. Using this technique temperature measurements have been made in a stoichiometric CH₄/N₂O flame above a sintered-bronze-flat-flame burner. The results in the burnt gas region are compared with those from (0,0) band reversal measurements on OH and Raman vibrational measurements on N₂. In addition to the fluorescence technique, a simultaneous absorption-fluorescence curve-fitting approach was also developed. The approach could be used for the simultaneous fit or for fitting either the absorption or fluorescence data individually. Good results were obtained using as few as two or as many as five transitions. Temperature profiles from fluorescence measurements in the (1,1) band and absorption measurements in the (0,0) band were compared. The agreement of results from all of the methods is good. In this paper a more detailed description of the apparatus and procedures is given than has appeared previously. The resulting flame temperatures are discussed in terms of flame chemistry and burner characteristics.

⁶Anderson, W.R., unpublished results.

II. EXPERIMENTAL

A diagram of the apparatus is shown in Fig. 1. The laser was a flashlamp pumped dye laser (Chromatix CMX-4) with intracavity etalon line narrowing and frequency doubling. The doubled output in the 3120-35 Å region was obtained by mixing Rhodamine 6G dye in Ammonyx LO and water. The measured bandwidth was 0.34 cm^{-1} in the ultraviolet (uv) using a scanning Fabry-Perot and the pulse duration was about 1 μsec . The maximum pulse energy used was about 0.3 mJ. The corresponding peak power was not sufficient to achieve saturation in an atmospheric-pressure flame as evidenced by linearity checks on the fluorescence signal. Output from the dye laser was separated by a dichroic splitter which reflected visible light and transmitted uv light. The visible light passed through a fixed etalon monitor used to confirm that lasing occurred on only one internal etalon mode. The uv light was transmitted through a Corning 7-54 filter which absorbed the residual visible light. A small portion of the uv light was reflected by a quartz window into a reference photodiode used to monitor power drifts. The main uv beam was focussed into the flame by an 11.4 cm lens. The light was recollimated by a second lens and a small portion was reflected into a second photodiode for transmission measurements. Fluorescence exiting the flame at right angles to the beam waist was focussed with 1:1 imaging on the slits of a 35 cm monochromator. The beam waist at the interaction region was about 200 microns in diameter. The length observed was 2.0 mm as determined by the monochromator slitwidth. The monochromator was centered at 3175 Å with a bandpass of about 36 Å. Outputs from the monochromator's photomultiplier and the transmission photodiode were ratioed to that from the reference photodiode in two separate boxcar averagers (PAR Model 162). Hard copy of the output was obtained on a strip chart recorder. For experiments in which curve-fitting data reduction techniques were used, a PDP 11/04 computer system (not shown) with A/D conversion was used for direct digitization of the boxcar outputs.

The burner used in these experiments was a water-cooled, sintered-bronze-porous-plug burner. The sintered portion was 5.72 cm in diameter. Two capillary flow regulators⁷ supplied the fuel and oxidant gases. Flow rates could be controlled to within 1%. The gases were 99% pure (Matheson) and were used without further purification. Supply gases were premixed inside the burner. An exhaust pipe placed over the flame stabilized the flame and removed noxious fumes. Burner heights were measured using a dial indicator gauge which was mechanically connected to the burner. Accuracy and reproducibility of the measurements was limited to 25 microns by the mechanical coupling. An estimate of the laser beam deflection resulting from refractive index gradients in the flame was obtained by examining the transmitted beam position several meters from the burner with and without the flame. The beam deflection was less than 50 μ through the entire flame even when passing through the flame front.

⁷DeWilde, M.A., "Capillary Flowmeters for Accurate, Stable Flows of Gases," BRL Technical Report No. ARBRL-TR-02230, 1980, AD A083874

LEF APPARATUS

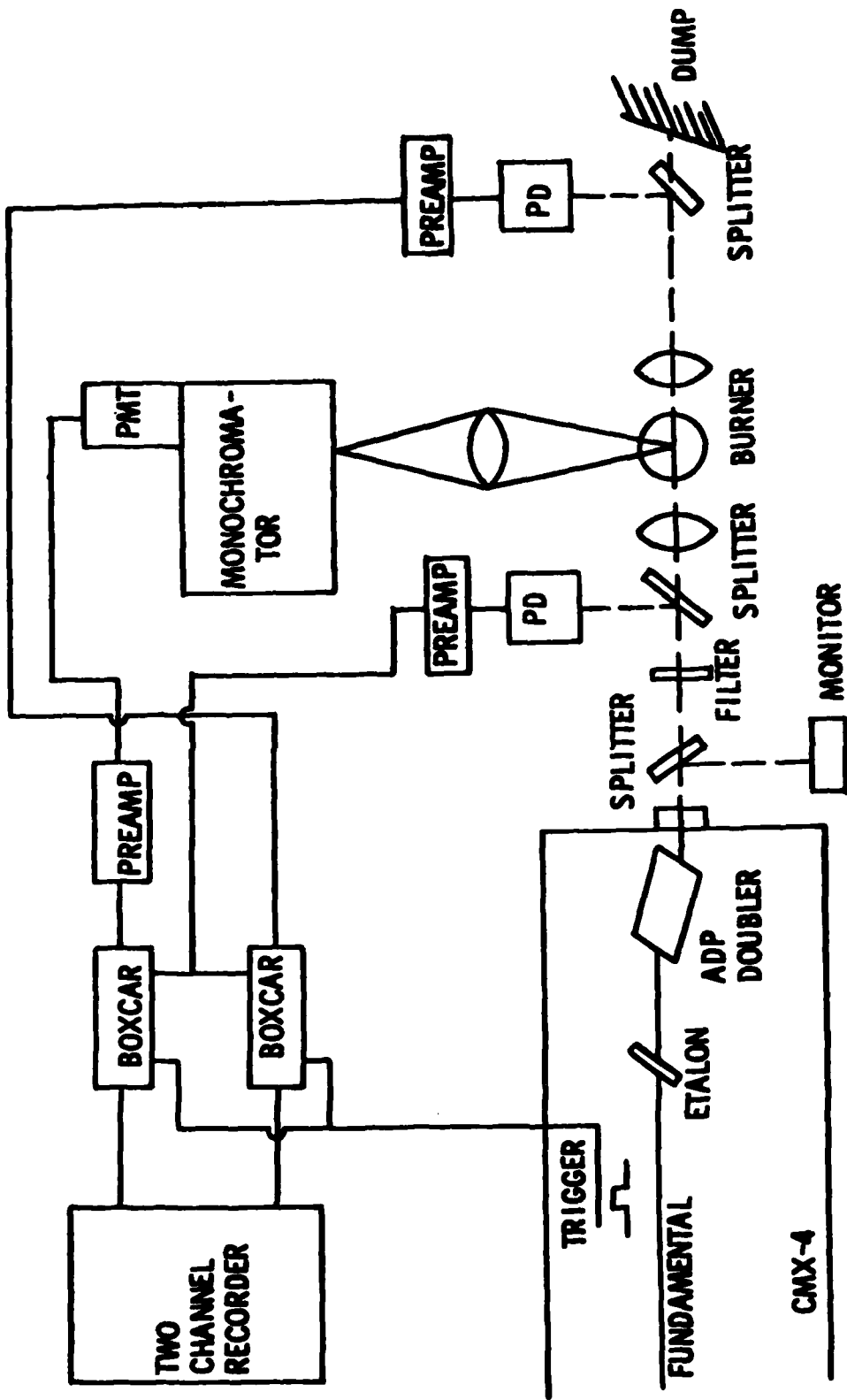


Figure 1. Experimental Apparatus. Frequency doubled radiation from a flashlamp pumped dye laser excites OH molecules above the burner. The first splitter and filter remove visible light from the beam. Small portions of the ultraviolet beam are reflected into two photodiodes to provide a reference and transmission signal. Fluorescence is viewed by a small monochromator. The various signals are processed and ratioed in two boxcar averagers.

III. RESULTS

Excitation scans across the (1,1) R-branch bandheads were run at several points above the center of the burner. In early runs, the laser was scanned from 3121 to 3135 Å. Nineteen (1,1) band lines in this region were sufficiently resolved that intensity measurements could be made without involved deconvolution calculations. All of these transitions are of comparable intensity so that the detector sensitivities did not have to be changed during a scan. These excitation transitions were in order of increasing wavelength: R_{18} , R_{17} , R_{15} , $R_{15'}$, R_{11} , $R_{14'}$, R_{12} , $R_{13'}$, R_{29} , R_{28} , R_{27} , R_{14} , R_{25} , R_{213} , R_{15} , R_{24} , R_{214} , R_{23} , R_{215} . (An $R_{1'}$ satellite in the notation used here is equivalent to the R_{21} transitions of Dieke and Crosswhite⁸. Line positions were obtained from Ref. 8). It was later found that the scan could be stopped at 3131 Å, which eliminates the last four transitions and considerably reduces run time, while yielding equivalent results. In addition, for one of the scans the $R_{19'}$, $R_{110'}$ and $R_{111'}$, which are quite weak satellites, were carefully amplified and measured to check for differences in response at these transitions.

A quick glance at Fig. 2, which is the OH (1,1) band R-branch excitation scan studied in this work, shows that (0,0) band transitions have quite strong absorptions while no (1,1) band transition has greater than 5% absorption which means the intensity at the focal point is reduced by no more than 2.5% by absorption. These limits were observed even at the highest OH concentration. Such small absorptions do not necessitate that corrections be applied for pump depletion.

Effects of self-absorption in the (0,0) band can be seen, qualitatively, by comparing the Q_{216} and P_{29} transitions. Although the absorption for the P_{29} is stronger, fluorescence from this excitation is weaker. (The fluorescence response overdrives the detection electronics, but comparative signal strengths may be estimated from widths at the overdrive point. The (1,1) band transitions overlapping the P_{29} do not significantly affect the absorption, while they can only increase the fluorescence). This effect undoubtedly results from peaking of the excited state rotational distribution near the state which is pumped⁴. Fluorescence lines resulting from this distribution connect to ground states having N'' nearly the same as N' , the ground and excited state rotational quantum numbers respectively. Therefore, one expects there will be more self-absorption of the fluorescence when transitions arising from levels near the peak in the ground state rotational distribution are pumped. Such is the case in Fig. 2 for the previously cited transitions having $N'' = 9$ and 16 since, as shall be seen, the ground state distribution peaks near $N'' = 6$ at the observed temperatures. In order to check for self-absorption in the (1,1) band, the fluorescence from one of the strongest lines was monitored while the burner was moved on a line towards the monochromator, i.e., perpendicular to the laser beam. The result is shown in Fig. 3. This horizontal profile was obtained 1 cm above the burner. The symmetry of the profile shows that self-absorption does not

⁸Dieke, G.H. and Crosswhite, H.M., "The Ultraviolet Bands of OH" *J. Quant. Spectrosc. Radiat. Transfer*, Vol. 2, p. 97, 1962.

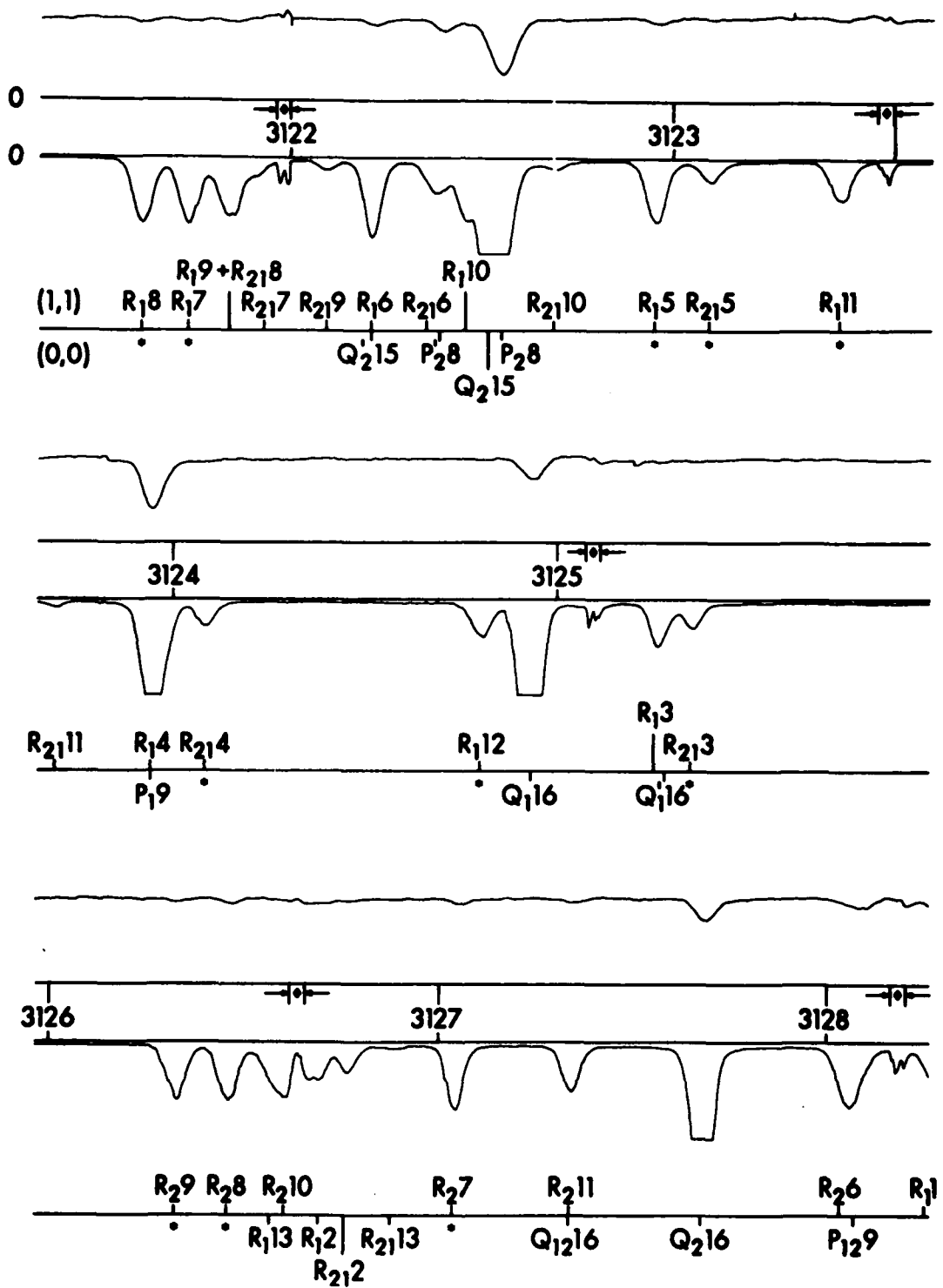


Figure 2. OH (1,1) band R-branch excitation scan in CH₄/N₂O Flame. Upper Trace: Transmission. Lower Trace: Fluorescence. Diamonds enclosed in arrows indicate laser etalon resets, an artifact of the scanning mechanism. Wavelengths are in angstroms.

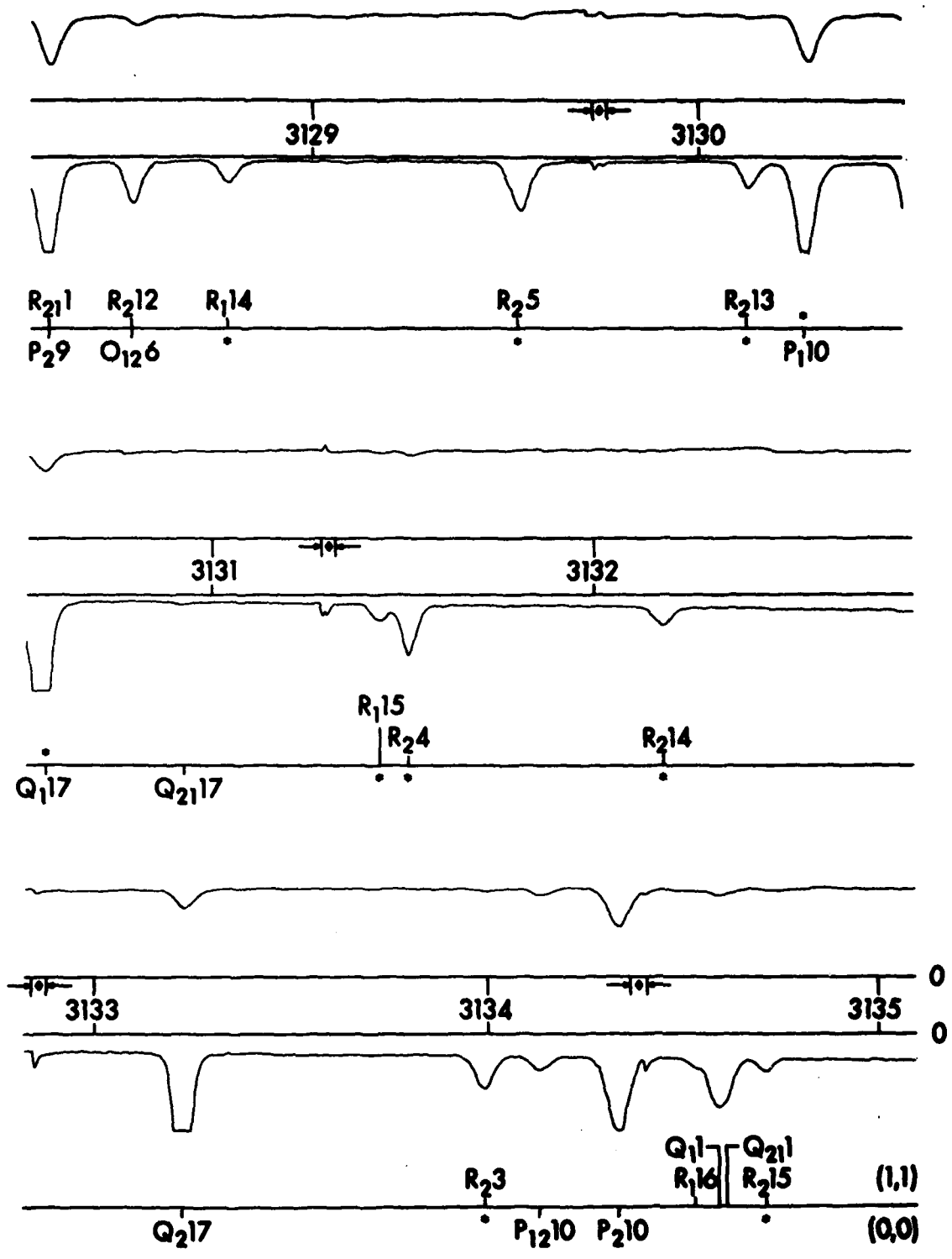


Figure 2.

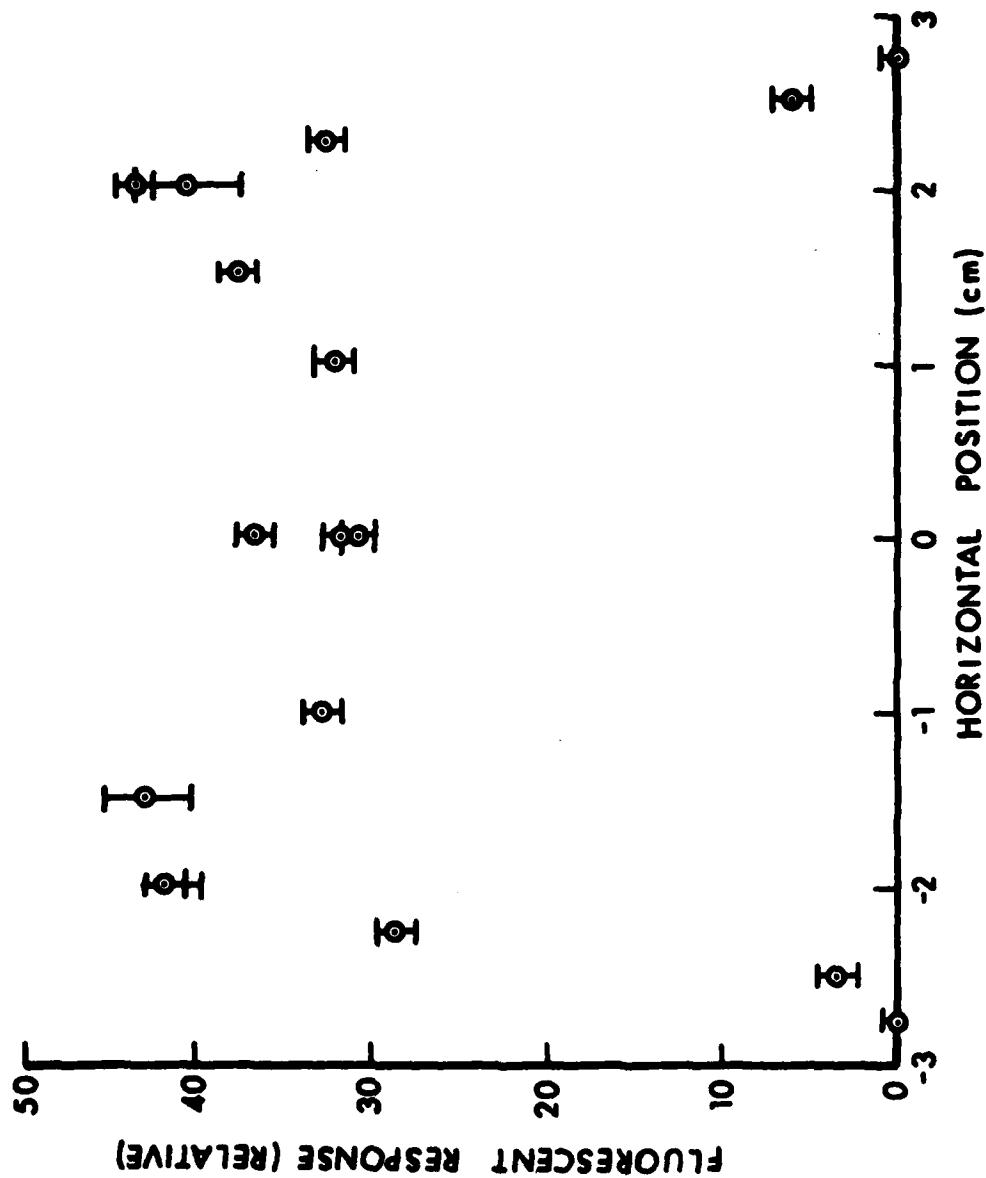


Fig. 3. Horizontal Fluorescence Profile of the (1,1) R₂₉ Transition of OH in CH₄/N₂O Flame at 1 cm Height. The burner is moved on a line towards the monochromator (perpendicular to the laser beam). At zero, the laser beam is centered over the burner. Positive numbers indicate burner motion towards the monochromator. Symmetry of the profile for this pumping transition, one of the strongest in the (1,1) band, indicates absence of self-absorption problems.

significantly affect (1,1) band fluorescence. Later studies⁹ have shown that the OH concentration at this height is within a factor of 2 of the peak concentration. The lack of appreciable laser beam absorption and an increase by only a factor of 2 at the highest density is proof that self-absorption in the (1,1) band is negligible for our flame.

The data reduction for temperature measurements is quite simple. It was noted that fluorescence peak widths in the (1,1) band did not vary within experimental error limits. Thus, we could assume the peak heights, which were easily measured from the chart recorder outputs, were proportional to the integrated line intensity. If one assumes the fluorescence yield within the bandpass of the monochromator is the same for all excited rotational levels pumped*, then the fluorescence intensity is proportional to the pump rate. Thus, for the fluorescence intensity normalized to the laser power, one has

$$I \propto B_{12} N_{N'',J''} \quad (1)$$

where B_{12} is the Einstein absorption coefficient for the appropriate transition, $N_{N'',J''}$ is the number density in the ground rotational state (N'',J'') and J'' is the total angular momentum quantum number in the ground state. If one further assumes the ground state is equilibrated, one has

$$N_{N'',J''} \propto (2J''+1)\exp(-E_{N'',J''}/kT) \quad (2)$$

where $E_{N'',J''}$ is the ground state energy, k is Boltzmann's constant and T is the rotational temperature. Combining Eq. (1) and (2), one finds

$$\ln[I/B_{12}(2J''+1)] = -E_{N'',J''}/kT + C \quad (3)$$

for some constant C . A typical plot of Eq. (3), from data taken 0.50 cm above the burner, is shown in Fig. 4. The Einstein B_{12} coefficients were obtained from Ref. 10 and the ground state rotational energies from Ref. 8.

*At first glance, this would seem to be equivalent to assuming that rotational redistribution in the excited state leads to nearly equivalent distributions no matter what state is pumped. However, this need not necessarily be the case.

⁹(a) Anderson, W.R., Decker, L.J. and Kotlar, A.J., "Measurement of OH and NH Concentration Profiles in Stoichiometric CH₄/N₂O Flames by Laser Excited Fluorescence," Paper 67, Eastern Section Fall Meeting of the Combustion Institute, Princeton, New Jersey, Nov. 1980. (b) Anderson, W.R., Kotlar, A.J., and Decker, L.J., "Concentration Profiles of OH and NH in a Stoichiometric CH₄/N₂O Flame by Laser Excited Fluorescence and Absorption," to appear in *Combustion and Flame*.

¹⁰(a) Chidsey, I.L. and Crosley, D.R., "Calculated Rotational Transition Probabilities for the A-X System of OH," *J. Quant. Spectrosc. Radiat. Transfer*, Vol. 23, p. 187, 1980. (b) Dimpfl, W.L. and Kinsey, J.L., "Radiative Lifetimes of OH ($A^2\Sigma^+$) and Einstein Coefficients for the A-X System of OH and OD," *J. Quant. Spectrosc. Radiat. Transfer*, Vol. 21, p. 233, 1979. (c) Goldman, A. and Gillis J.R., "Spectral Line Parameters for the A $^2\Sigma - X^2\Pi$ (0,0) Band of OH for Atmospheric and High Temperatures," submitted for publication.

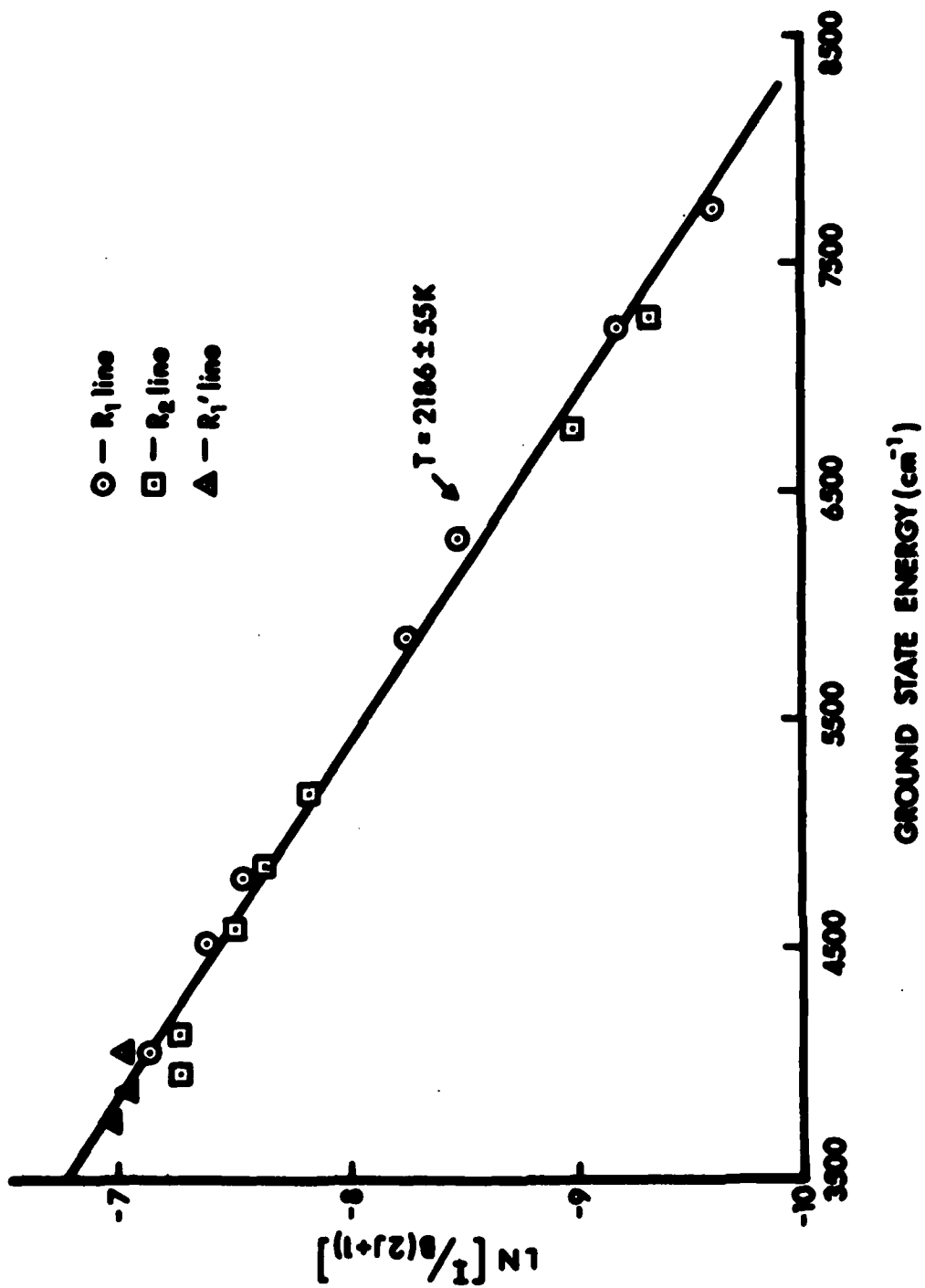


Fig. 4. Boltzmann Plot for a Typical Fluorescence Excitation Scan of the OH (1,1) Band in CH₄/H₂O Flame.

A curve-fitting routine was developed to separately or simultaneously fit the absorption and fluorescence data. For curve fitting of absorption spectra, five lines which are fairly close to one another in the spectrum were used. These were the Q₁₁₇ and P₁₁₀ from the (0,0) band and R₂₄, R₁₁₅ and R₂₁₃ from the (1,1) band. For curve-fitting of fluorescence data only the three (1,1) lines could be used because of obvious absorption problems for the (0,0) band data. The lineshapes were fitted using a least squares computer program which accounts for a Gaussian laser profile, Doppler and collisional broadening of the transition, the number density, which is considered in more detail in Ref. 9b, and the temperature. The theory is covered in more detail in the appendix. The approach is an extension of an earlier single transition technique for the determination of concentration and temperature from absorption data by Lück and Müller¹¹ for lasers with bandwidths much narrower than the transition bandwidth. (In this paper, reduction of fluorescence data was accomplished by two different methods. Unless the curve-fitting approach is specifically mentioned, the peak height - Boltzmann plot approach was used to extract the temperature).

The temperature profile of the stoichiometric CH₄/N₂O flame is shown in Fig. 5. Fig. 5a shows results of Boltzmann-plot fluorescence measurements taken up to 2.5 cm above the burner. Fig. 5b compares the results of Boltzmann-plot fluorescence measurements to some of our earliest absorption curve-fitting measurements taken in the first 1.0 mm above the burner. In these early absorption curve-fitting measurements, only data from the two (0,0) band lines was used to extract the temperature.* Also shown are the adiabatic flame temperature, resulting from a thermochemical equilibrium calculation¹², and the burner head temperature, which is of interest for flame modeling. The burner head temperature was extrapolated from thermocouple measurements along the outside of the burner body, as shown in Fig. 6. As can be seen, the temperature is nearly constant, within $\pm 3^\circ\text{C}$, up to 1 cm below the top of the burner, and then falls off rapidly. Since the porous-plug portion of the burner is 1.85 cm thick, the rest of the burner being essentially a hollow cylinder, it is not surprising that the temperature is nearly constant in this portion of the burner, nor is it unreasonable to assume the gas temperature is the same at the burner surface.

* Note that very precise measurements are possible with the curve fitting technique because about 100 points per transition are fitted. Lower precision is attained if only the value at linecenter is used as in the Boltzmann-plot fluorescence approach.

¹¹Lück, K.C. and Müller, F.J., "Simultaneous Determination of Temperature and OH Concentration in Flames Using High Resolution Laser-Absorption Spectroscopy," *J. Quant. Spectrosc. Radiat. Transfer*, Vol. 17, p. 403, 1977.

¹²Svehla, R.A. and McBride, B.J., "Fortran IV Computer Program for Calculation of Thermodynamic and Transport Properties of Complex Chemical Systems," NASA TN-D-7056, 1973.

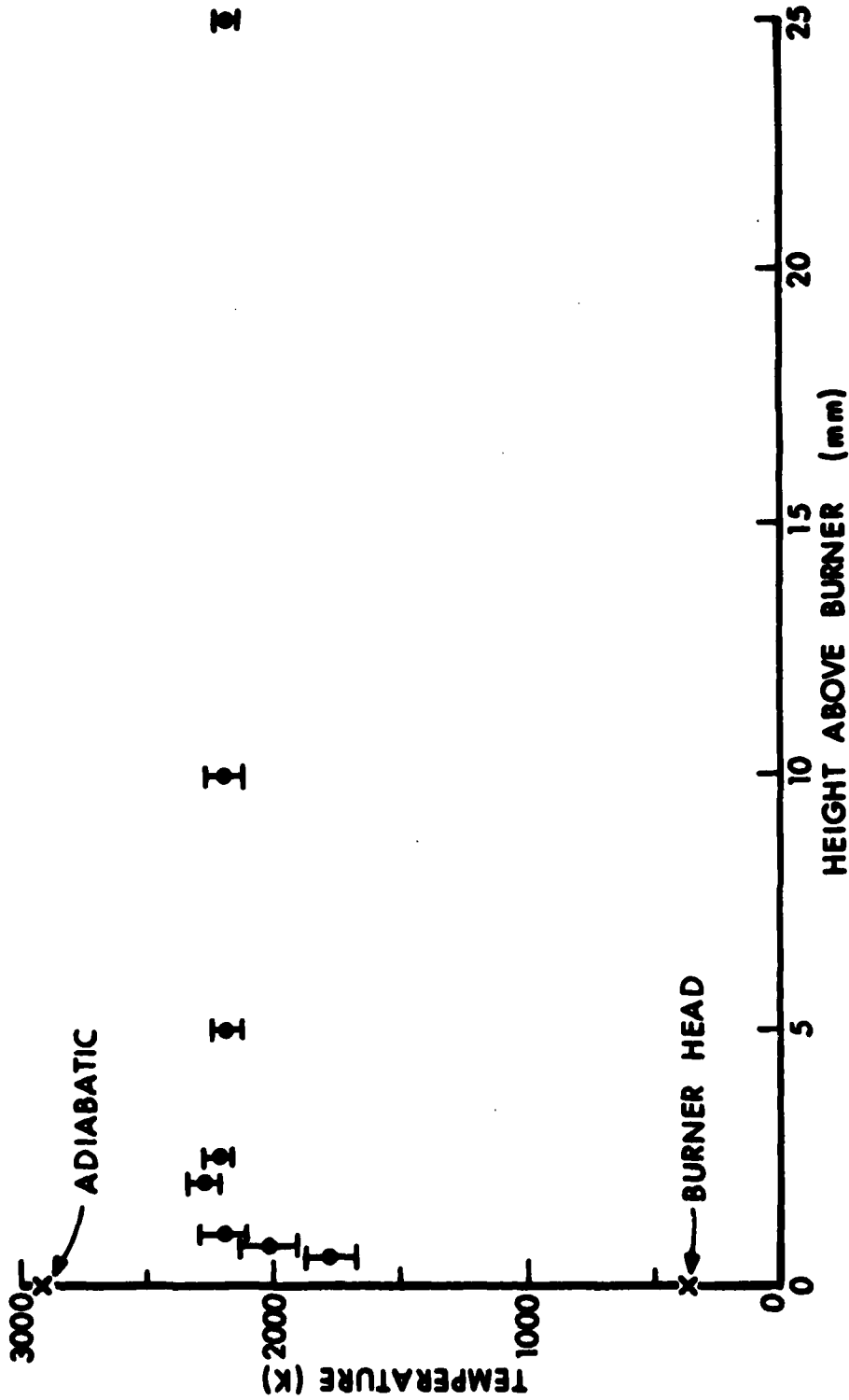


Figure 5. Vertical Temperature Profile in a Stoichiometric $\text{CH}_4/\text{N}_2\text{O}$ Flame. a. Fluorescence results showing nearly constant temperature in the burnt gas region. The calculated adiabatic and measured burner head temperatures are also indicated.

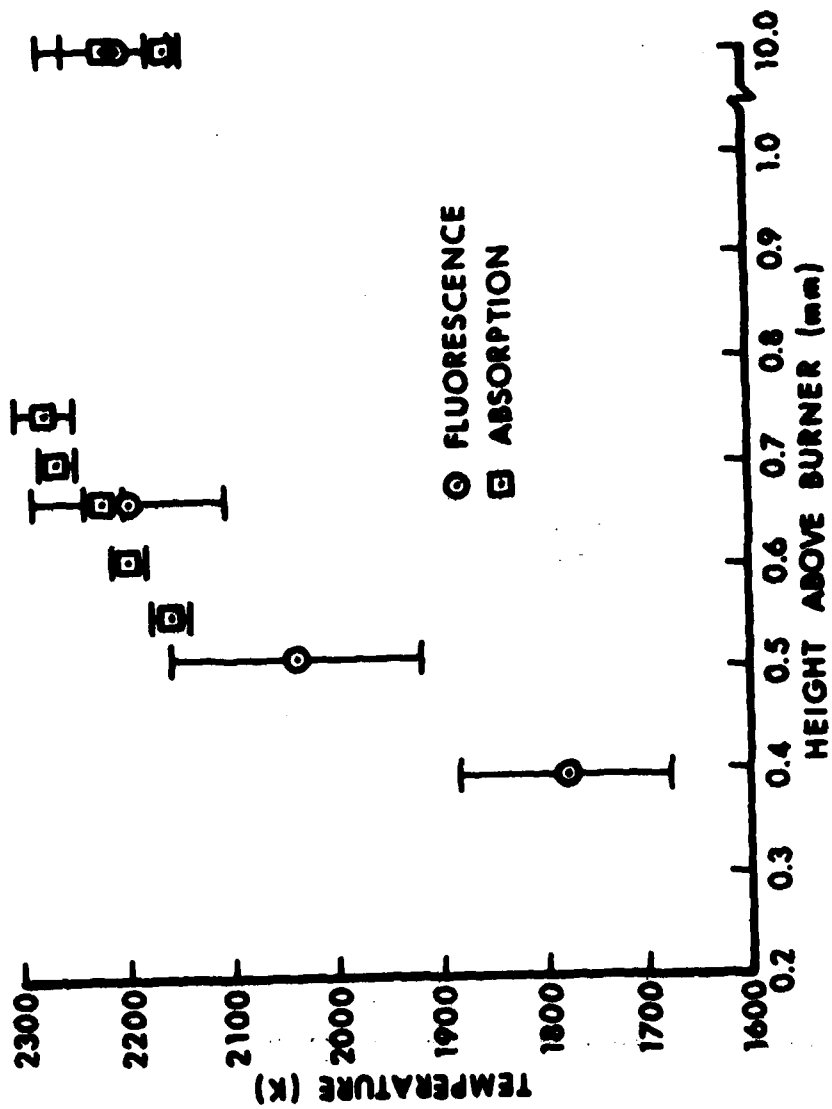


Figure 5b. Comparison of absorption and fluorescence results showing the rapid climb in the first millimeter and temperature at 10 millimeters.

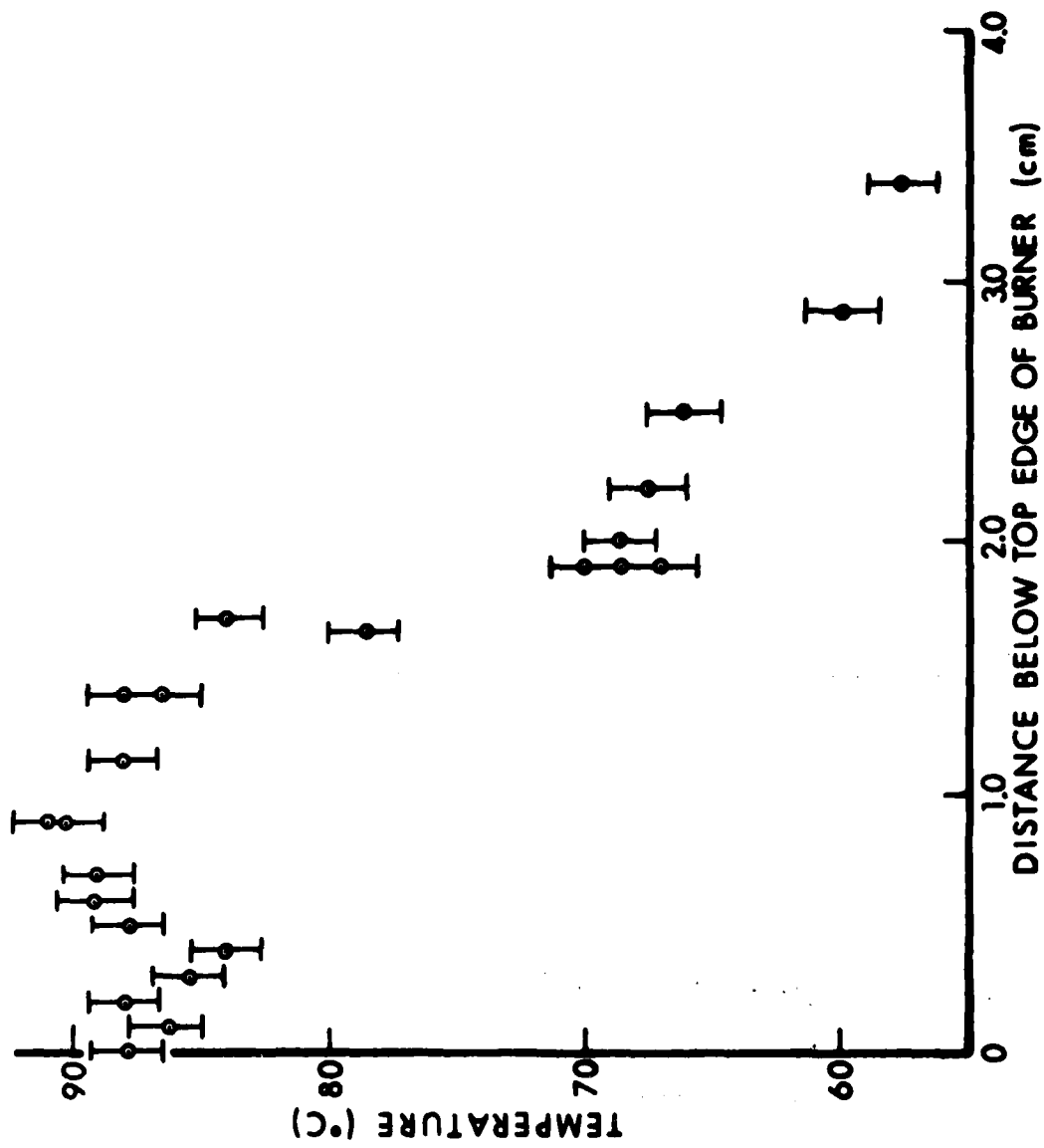


Figure 6. Burner Body Temperature at Several Points Below the Edge of the Burner Head. The sintered portion of the burner is 1.85 cm thick, accounting for the nearly constant temperature in that region.

It was of interest to examine the curve-fitting approach in more detail for two reasons. First, it was noted that the (1,1) R₂₁₃ lies in close proximity to the (0,0) P₁₁₀. There was thus a concern that ignoring the effects of its presence, as was done in deriving the absorption data of Fig. 5b, might result in systematic errors in the temperatures. To examine this possibility, two scans across the five transitions were made in the burnt gas region of the flame, 1 cm above the burner. The data set was then restricted to wavelengths containing the three transitions of interest, namely the two (0,0) lines and the (1,1) R₂₁₃. The absorption data was then fitted by both including and excluding effects of the (1,1) R₂₁₃ on the spectrum. For the individual runs, no difference, within error limits, was found for extracted temperatures (or densities) whether effects of the (1,1) R₂₁₃ were considered or not. This result is reasonable since absorption by the (1,1) R₂₁₃ is weak. The absorption results of Fig. 5 are therefore not affected by ignoring effects of this transition.

The second reason for examining the curve-fitting approach in more detail is the following. It is possible that fluorescence yields from individual transitions as measured by the monochromator systematically differ. However, they might differ in a random fashion such that the temperature derived from Boltzmann plots, as in Fig. 4, is unaffected. The systematic differences would then appear as random scatter. On the other hand, if only a few transitions are considered the derived temperatures are more likely to be affected by the systematic errors. To check this possibility three curve-fitting procedures were used on the two data sets mentioned in the last paragraph. The two scans of course provided fluorescence data as well as absorption data. In the first curve-fitting approach, the fluorescence data was ignored and the two (0,0) and the (1,1) R₂₁₃ absorption peaks were fitted. In the second approach, the absorption data was ignored and the three (1,1) band fluorescence peaks were fitted. In the last approach, the three (1,1) fluorescence peaks and all five absorption peaks were fitted simultaneously. Fluorescence yields for the three (1,1) transitions in the second and third approach were treated in a special way. The R₂₄ and R₁₁₅ fluorescence yields were forced to be equal while that for the R₁₁₃ was allowed to be different.* One of the scans and the computer fit using the third approach is shown in Fig. 7. Quality of the fits using the other two approaches is similar to that in Fig. 7.

The resulting temperatures for the three approaches and the data set of Fig. 7 were $2164 \pm 11\text{K}$, $2201 \pm 15\text{K}$, and $2166 \pm 10\text{K}$, respectively. The other scan yielded $2215 \pm 17\text{K}$, $2150 \pm 16\text{K}$, and $2203 \pm 13\text{K}$, respectively. Parameters from the two runs were then combined in such a way that diagnostic parameters, such as temperature and number density which should be the same for the two runs, were constrained to be the same, while other parameters, such as baseline positions, were allowed to be different. The resulting values are the best estimates for the parameters at the given point in the flame. The temperature thus found for the first technique, absorption fit, was $2179 \pm 21\text{K}$. The temperature for the third technique, simultaneous absorption-fluorescence fit was $2179 \pm 19\text{K}$. A similar combination was not performed for results from fluorescence data only. Note the temperatures found were near the

* Because the optically thin limit was not used for the calculation, the R₂₄ and R₁₁₅ transitions, which overlap, could not be decoupled. Their fluorescence yields were therefore assumed to be equal. The quality of the fit, Fig. 7b, is a measure of the validity of this assumption.

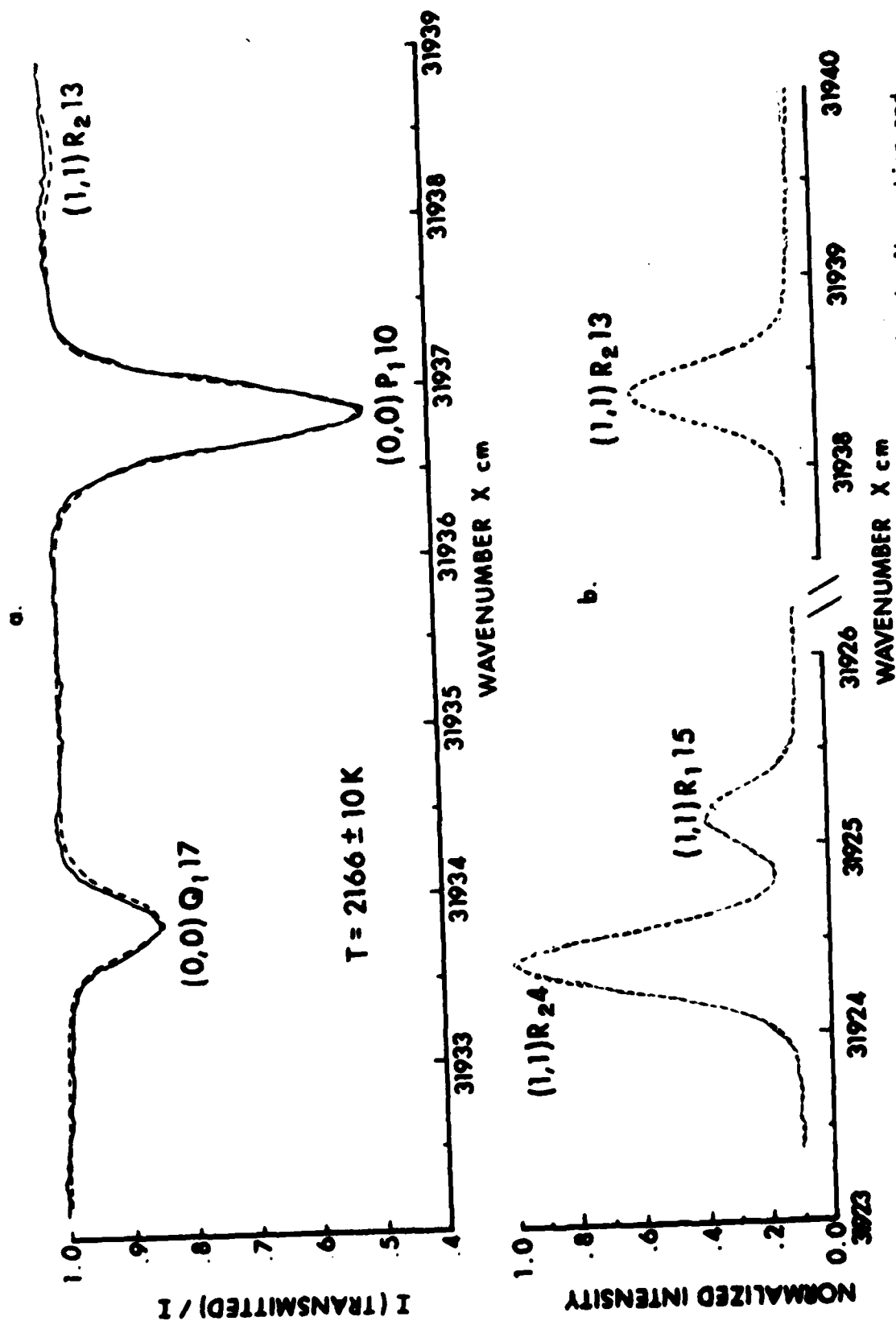


Figure 7. An Example of Data Used for Simultaneously Fitting Five Lines in the Absorption and Fluorescence Spectra of OH. (a) Absorption spectrum. Two of the (1,1) transitions which were included in the fit are not shown. (b) Fluorescence spectrum. Solid lines - experimental data. Dashed lines - computer fit.

average from the fits of the individual runs. As can be seen, the true precision of each of the curve-fitting methods for individual data sets is somewhat lower than the statistical result, possibly because of some slight drift in burner conditions or detector stabilities of a duration equivalent to single peak scan times. In spite of this problem, the agreement among the methods is quite satisfactory. The results agree extremely well with those from the simpler fluorescence peak height - Boltzmann plot approach and the two-line absorption curve-fitting approach at 1.0 cm (see Fig. 5). Note that there is reasonable agreement between results of techniques 1 and 2. We also found that the two fitted fluorescence yields for the three (1,1) transitions were always nearly equal. Though this study was by no means exhaustive, it would thus appear that randomly scattered differences in fluorescence yields are quite small using our arrangement.

Besides the fluorescence and absorption measurements on OH, reversal measurements on the OH (0,0) band R-head at 3064 Å¹³ and Raman vibrational band temperature measurements on the Stokes Q branch of N₂¹⁴ have also been performed at 1 cm. The reversal measurements were similar to Na D-line reversal measurements¹⁵ except that flame seeding is not required. A tungsten lamp gave sufficient intensity to achieve reversal at 3064 Å, but the spatial resolution was only about 1 cm. Therefore, measurements had to be confined to the burnt gas region. The LEF results in Fig. 5a indicate that the temperature is almost constant so that the reversal measurement is not affected by spatial gradients. The results are compared with those from LEF measurements at 1 cm above the burner in Table 1. As can be seen, the agreement is excellent. The flame temperature peaks near the stoichiometric mixture, as one would expect¹⁶. The Raman and LEF results were compared both on the porous plug burner and on a small slot burner. For the stoichiometric flame, 1 cm above the porous-plug burner the Raman measurements yielded 2141 ± 26K, in reasonable agreement with the fluorescence measurement (see Table 1). A measurement by both techniques at the same point above the slot burner flame, which cools the flame less, yielded a Raman N₂ temperature of 2600 ± 50K while the OH LEF temperature was 2530 ± 110K.

¹³ Anderson, W.R., "Measurement of the Line Reversal Temperature of OH in CH₄/N₂O Flames," BRL Technical Report No. ARBRL-TR-02280, January 1981 (AD A095349)

¹⁴ Beyer, R.A. and Vanderhoff, J.A., "Raman Spectroscopy of Premixed CH₄/N₂O Flames," BRL Report, to be published.

¹⁵ Snelleman, W., "Errors in the Method of Line-Reversal," *Combustion and Flame*, Vol. 11, p. 453. 1967, and Ref. 16.

¹⁶ Gaydon, A.G. and Wolfhard, H.G.W., "Flames: Their Structure, Radiation and Temperatures," Chapman and Hall, LTD., London, 1970.

Table I. Comparison of LEF Excitation Scan and Band Reversal Measurements of Temperature in CH₄/N₂O Flames.

Eq. Ratio $\phi = 4[\text{CH}_4]/[\text{N}_2\text{O}]^a$	Temp. (K) from LEF of OH	Temp. (K) from OH Band Reversal
1.18	2113 \pm 38	2129 \pm 50
1.01	2199 \pm 53	2194 \pm 45
0.55	not measured	2089 \pm 70

^aFor the stoichiometric flame, the total premixed gas flow rate was 9.96 \pm 0.10 l/min (298 K). For the other flames, the oxidant flow rate was held constant and the fuel flow rate changed until the equivalence ratios reported were achieved.

IV. DISCUSSION

A. Diagnostic Considerations

As can be seen from a comparison of the temperatures obtained by the various methods, the fluorescence technique yields quite accurate results. Agreement between Raman, fluorescence, absorption, and band reversal techniques for regions having significantly different temperatures on two different burners shows that the compatibility of the results is not merely due to a fortuitous agreement for the conditions in the burnt gas region above the porous-plug burner where most of our early measurements were performed. This result lends credence to the lower LEF temperatures observed in the flame front where comparison measurements could not be performed by all the techniques.

The excellent agreement between the fluorescence data and the Raman, absorption and band reversal results does not support the predictions of the fluorescence model developed by Smith and Crosley^{4b,d}. The model considers the effects of competition between rotational energy transfer collisions in the $v' = 0$ state and electronic quenching. In their experiments, the OH in a CH₄/air flame was excited. Rotationally resolved fluorescence scans were run upon pumping several different transitions. From this data, information concerning the energy transfer within the $A^2\Sigma^+$ state could be deduced. For transfer in which the spin state remains unchanged ($\Delta N' = \Delta J'$ where J' is the total angular momentum quantum number of the excited state) the rotational distributions were peaked near the rotational level pumped by the laser with considerable densities in nearby states. Only the populations of rotational levels far removed from the initially pumped level ($\Delta N' > 3$) did not exhibit this peaking effect. Levels well below the initially pumped level in energy contained equal densities, except for a degeneracy factor, while populations in those above it could be represented by a Boltzmann distribution. The temperature characterizing this distribution does not reflect the actual equilibrium temperature of the system but depends on which rotational level is pumped. For transfer involving a change of spin state ($\Delta N' \neq \Delta J'$) the entire distribution was characterized by the same temperature as the high energy states for which $\Delta N' = \Delta J'$. However, there was an overall lower propensity to change spin states, that is, the density of the opposite spin component to that initially pumped lay below that for the same spin state on the Boltzmann plots.

The implication of the results of Ref. 4 is that a narrow bandwidth detector will discriminate for or against the level pumped, depending upon where the detector is centered, owing to the differences in rotational distributions as the pumped level is changed. In most experiments, the detector is centered on or near a bandhead of OH. One would therefore expect a higher fluorescence yield when a state at or near states radiatively connected to transitions in the bandhead is pumped. Conversely, pumping states whose transitions lie far away from the bandhead would lead to low fluorescence yields. The lower rotational quantum number transitions are, generally, closer to their respective bandheads than high ones so the detector is expected to increasingly discriminate against transitions as N' increases. Thus, one predicts the measured temperature from fluorescence scans with narrowband detectors will usually be lower than the actual value. The model of Crosley and Smith for (0,0) band work with a bandwidth of 30 Å

predicts that temperatures can be systematically low by several hundred Kelvins. For (1,1) band work, even poorer accuracy is expected¹⁷. The flame composition of CH₄/N₂O and CH₄/air flames in the burnt-gas region is similar enough that the disagreement between the two studies cannot be attributed to differing flame characteristics.

Earlier results on CH₄/N₂O in this laboratory^{5a} yielded higher temperatures than reported here. Also, there was a systematic difference in fluorescence yields for R₁, R₂ and R₁' transitions (especially R₁'9, 10 and 11) as revealed in the Boltzmann plots. The early resulting differences in fluorescence yields were thought to support the model of Smith and Crosley which predicts possible differences in fluorescence yield for F₁ and F₂ spin states. However, a systematic drift in premixed gas flow rates was later found and corrected. The difference in fluorescence yields on Boltzmann plots disappeared (c.f. Fig. 4) and resulting temperatures were slightly lower. The previous result is, therefore, inaccurate and does not lend support to the model of Smith and Crosley as was originally thought in Ref. 5a.

The v' = 1 to 0 vibrational transfer in the excited state may significantly affect the present experimental results. Such transfer reduces the fluorescence yield if the detector views (1,1) band transitions as in the present work. Studies involving OH in pure gases^{18a,19} and in CH₄/air flames^{18b} indicate that the rate of vibrational deexcitation drops as the rotational quantum number, N', increases. This effect could compensate for the aforementioned rotational transfer effects, evening out the fluorescence yields for the different rotational levels. The effect is not included in the model of Smith and Crosley.

The results of Cattolica² in the (0,0) band and of Bechtel³ in both the (0,0) and (1,0) band, with narrowband detectors in the (0,0) band, also show quite good agreement with other methods of temperature measurement as long as absorption problems are not too severe. The agreement in these cases cannot be explained by the rotational dependence of the vibrational transfer rate, as it might be for the (1,1) band, since the (0,0) band fluorescence should hardly be affected and results of pumping in the (1,0) band with (0,0) band detection should be even poorer because of the effect. There appears to be little dependence of the electronic quenching rates on the rotational quantum number¹⁹ so this effect would not explain the accuracy of the results either. The experimental parameters used in the various (0,0) band studies are summarized in Table 2.

¹⁷ Crosley, D.R., private communication.

¹⁸ (a) Lengel, R.K. and Crosley, D.R., "Energy Transfer in A²Σ⁺ OH. II. Vibrational", *J. Chem. Phys.*, Vol. 68, p. 5309, 1978. (b) Crosley, D.R. and Smith, G.P., "Vibrational Energy Transfer in A²Σ⁺ OH in Flames," Paper 69, Eastern Section Fall Meeting of the Combustion Institute, Princeton, New Jersey, Nov. 1980.

¹⁹ German, K.R., "Collision and Quenching Cross Sections in the A²Σ⁺ State of OH and OD," *J. Chem. Phys.*, Vol. 64, p. 4065, 1976.

Table 2. Experimental Parameters in Previous (0,0) Band LEF Temperature Determinations.

<u>Reference</u>	<u>Bandcenter (Å)</u>	<u>Bandpass (Å, FWHM)</u>	<u>N' Range^a</u>
Cattolica [2]	3090	35	2-8
Bechtel [3]	~ 3070 ^b	~ 12.5	~ 1-16
Crosley and coworkers, experi- ment [4]	3090	13.5	~ 1-12
	3090	250	~ 1-12
Crosley and coworkers, model [4]	3070	30	1-15
	3090	30	1-15

^aFor Ref. [3] and for the experiment of Ref. [4], N' was not given. N'' was determined from the energy scale on the Boltzmann plots, using the energy level tables of Ref. [8], and is reported in this table in place of N'. N' must be within ±2 of N''.

^bApproximate position of R₁ and R₂ bandheads observed by Bechtel. The exact position of the bandcenter used in his experiments was not stated.

Results of the model^{4b,d} with a 3090 Å bandcenter indicate that measured flame temperatures can be quite low using narrowband detection. For a wideband detector, say 250 Å FWHM, the results can be quite accurate. This trend seems to be substantiated by Crosley and coworkers' experiments in which the measured temperature of a CH₄/air flame using narrowband detection was ~ 700K lower than with wideband (250 Å FWHM) detection. Unfortunately, corroboration by other techniques was not available. Crosley and coworkers state the model predicts similar results for a 3070 Å bandcenter. Also, the model predicts that much more accurate results will be observed if the excited levels N' = 3 to 9 are used (an assumed flame temperature of 1800K leads to an observed temperature of 1650K) rather than N' = 1 to 15. (assumed 1800K leads to observed 1400K) for the narrowband experiment at 3090 Å bandcenter. As can be seen in Table 2, the parameters in Cattolica's and Bechtel's experiments closely approximate those used in the model. Bechtel's bandpass is narrower than assumed in the model, but this should lead to even poorer agreement with the actual value than the model predicts. Yet, the results in these experiments are much more accurate, as confirmed by N₂ spontaneous Raman and thermocouple measurements, than the model predicts they possibly can be. Also, the (slight) curvature in Bechtel's Boltzmann plot is in the opposite direction to that which would be necessary to produce a higher temperature if only N' = 3 to 9 levels are considered. We can presently offer no explanation for these puzzling differences.

In addition to excitation scans on OH, a recent study of OH and NH concentration profiles was performed in this laboratory⁹. An NH (0,0) band R-branch excitation scan was recorded as part of this work. The corresponding Boltzmann plot exhibited very high fluorescence yields when states near those leading to transitions within the monochromator bandpass, which looked mainly at N' = 1 and 2 states, were pumped. These high yields are undoubtedly due to peaking in the rotational distribution near the state pumped as observed by Crosley and coworkers for OH. For those states, however, which are far removed from N' = 1 and 2, the Boltzmann plot yields a straight line and temperature, 2210 ± 120K, in good agreement with OH scans which yield 2040 ± 120K at the same point in the flame! It is clear more work needs to be done to explain the differences in the model's predictions and experimental results for OH and this surprisingly good result for NH.

The necessity of checking for absorption problems in fluorescence work, especially for OH which is present in high concentrations in most flames, is clearly demonstrated in this work. The (1,1) band excitation method is shown to be capable of avoiding such problems which must be considered in experimental design. If, for instance, it is desired to use even larger burners or higher pressures than used here, problems could ensue even for the (1,1) band. One might then attempt to use even higher vibrational levels. However, predissociation in the higher states²⁰ could complicate data reduction. The (1,1) band technique also needs to be studied at low pressures where energy transfer effects could significantly change.

²⁰ Sutherland, R.A. and Anderson, R.A., "Radiative and Predissociative Lifetimes of the A²Σ⁺ State of OH," *J. Chem. Phys.*, Vol. 58, p. 1226, 1973.

Effects of absorption can be seen in some of the previous OH excitation scans. The first such scan in a flame was reported in 1974 by Wang and Davis¹. In their research, Wang and Davis scanned the (1,0) band and observed fluorescence in the (0,0) band using a Bunsen burner. The technique demonstrated the feasibility of laser fluorescence experiments in flames, but unfortunately the derived temperatures were not checked using other techniques. Wang and Davis presented two measurements, one near the edge of the flame of 1100 K and one near the center where the Boltzmann plot exhibits two nearly straight line portions with differing slopes. The latter plot has a minimum at the middle of the energy abscissa. Previous workers^{2,4} suggested this departure from linearity could result from saturation effects. However, the power level* of 6.4×10^7 watts/cm² cm⁻¹ used in Wang's work is not high enough to cause significant saturation. The saturation studies of Lucht, et al.²¹ seem to indicate that even higher power levels are required before significant nonlinearities occur. Lucht, et al. were also pumping a stronger transition. Wang and Davis' observation of linearity of fluorescent intensity with laser power for the strongest transition studied further indicates the results are not affected by saturation. The (1,0) band has only a slightly smaller transition strength than the (0,0) band used in early Bunsen burner studies in this laboratory⁶, wherein strong absorptions were noted. It is quite likely the data from Ref. 1 taken at the flame center, and perhaps at the edge as well, is exhibiting effects of absorption. Therefore, no conclusions regarding energy transfer effects or ground state rotational populations can be drawn from Ref. 1.

In Cattolica's (0,0) band work², a flat-flame burner similar to the one in the present work was used. Cattolica found good agreement between N₂ vibrational Raman, thermocouple and fluorescence measurements near the edge of the flame, but not in the center. A horizontal fluorescence profile, similar to the one in Figure 3, was decidedly nonsymmetric. It was obvious absorption problems affected results in the center but not the edge of the flame. However, for both positions in the flame, straight-line Boltzmann plots were obtained. It is thus clear that straight-line fits do not indicate an absence of problems.

Cattolica has recently developed a two line fluorescence technique involving only satellite transitions of the (0,0) band²², which cause small, correctable laser depletions. The transitions he used pump the same excited state so that self-absorption and fluorescence bandpass effects (if nonnegligible) cancel. Unfortunately, the method requires extremely precise data since the temperature is essentially determined by only two points. A mini-computer system is a practical equipment to achieve this precision. Bechtel³ avoided absorption problems by using a burner which produces a curved flame front. A

* A typo appears in this quantity in Ref. 2.

²¹ Lucht, R.P., Sweeney, D.W. and Laurendeau, N.M., "Saturated Fluorescence Measurements of the Hydroxyl Radical," in Laser Probes for Combustion Chemistry (D.R. Crosley, ed.), ACS Symposium Series 134, American Chemical Society, Washington, D.C., 1980, p. 145.

²² Cattolica, R.J., "OH Rotational Temperature from Two-Line Laser Fluorescence," Appl. Opt., Vol. 20, p. 1156, 1981.

significant amount of laser absorption was seen when flat flames were used. The absorption in fact was used to calibrate fluorescence concentration profiles. The burner used in his work could be difficult to model and flashback occurs easily for fast flames. Each of the three approaches to absorption problems thus has advantages over the others which should be considered when tailoring an experiment.

B. The $\text{CH}_4/\text{N}_2\text{O}$ Flame

The temperature measured in the burnt gas region above the porous-plug burner, ~ 2200 K, is much lower than the adiabatic flame temperature, 2922 K, calculated using the thermodynamic equilibrium code¹². The lower temperature apparently results from cooling by the burner and not from incomplete burning as might occur if, for example, large amounts of NO were formed. Raman measurements on N_2 using a second slot burner, which cools the flame very little, show the temperature near the burner surface, just above the flame front, is very close to the adiabatic flame temperature¹⁴. Measurements of the inlet and outlet water temperatures and flow rate on the porous plug burner yield a cooling rate of 10.6 ± 1.0 kcal/min. Using the flow rate of 9.96 ± 0.10 l/min of the fuel gases at 298 K, one calculates a mass flow rate of 15.5 g/min. The thermochemical equilibrium calculation was forced to selected final temperatures 100 K apart to determine the equilibrium concentration and, hence, the heat capacity of the products as a function of temperature. The heat capacity function, multiplied by the mass flow rate, was integrated over temperature from 2922 K to lower temperatures until a temperature was reached such that the observed heat extraction rate by the water was matched*. The final temperature thus calculated was 2240 ± 100 K, in excellent agreement with the measurements in the burnt gas region. Of course, this does not prove the gases burn all the way to completion, though they must come close, nor does it preclude formation of small amounts of compounds thought to be nonreactive energy sinks above their equilibrium concentrations, such as NO. It does show the results are compatible with the adiabatic flame temperature.

As can be seen from Fig. 5, the temperature profile in the burnt gas region is nearly a horizontal straight line. This is unexpected since in this region, slow three-body radical recombinations release heat and slowly increase the temperature. However, some diffusion of room air into the flame could account for the constant temperature.

In addition to the vertical temperature profile measured above the center of the burner, a fluorescence temperature measurement was made 1 cm above the burner, and 1 cm from the edge, very near the maxima in the horizontal fluorescence profile of Fig. 3. N_2 Raman measurements at 1 cm height have also been made at several points, profiling the temperature drop as the beam is moved out of the flame into room air¹⁴. These measurements show the temperature is nearly constant at ~ 2200 K up to 2 mm from the burner edge and drops precipitously as one moves further away from this point towards the edge into room air. Therefore, the fluorescence profile in Fig. 3, except for some edge

* Note the dissociation of the products, an important effect, is automatically taken into account by this procedure since heat capacities from the equilibrium code contain a term for heats of dissociation.

corrections, is a true reflection of the relative OH number density. The increased OH density at the edge of the burner possibly results from some diffusion of O_2 in the room air into the flame. It is also conceivable that some cylindrically symmetric nonuniformity in the porous-plug burner leads to this effect.

V. CONCLUSIONS

The temperature profile in a stoichiometric CH_4/N_2O flame above a large porous-plug burner was measured using laser excited fluorescence of the OH radical. A new approach using the (1,1) band has been shown to eliminate the absorption problems in this flame and should be generally applicable for OH measurements in other flames. Comparison with OH reversal, N_2 vibrational Raman and OH laser absorption shows that the LEF technique is of comparable accuracy. Large amounts of absorption were found in (0,0) band work. This absorption is advanced as the cause of the non-Boltzmann population distributions which were obtained in previous work for the ground electronic state of OH.

REFERENCES

1. Wang, C.C. and Davis, Jr., L.I., "Ground State Population Distributions of OH determined with a Tunable UV Laser," Appl. Phys. Lett. Vol. 25, p. 34, 1974.
2. Cattolica, R.J., "OH Rotational Temperature from Laser Induced Fluorescence," Sandia Report No. SAND 78-8614, 1978.
3. Bechtel, J.H., "Temperature Measurements of the Hydroxyl Radical and Molecular Nitrogen in Premixed, Laminar Flames by Laser Techniques," Appl. Opt., Vol. 18, p. 2100, 1979.
4. (a) Smith, G.P., Crosley, D.R. and Davis, L.W., "Rotational Population Distributions in Laser-Excited OH in an Atmospheric Pressure Flame," Paper 3, Eastern Section Fall Meeting of the Combustion Institute, Atlanta, Georgia, 1979. (b) Smith, G.P. and Crosley, D.R., "Quantitative Laser-Induced Fluorescence in OH," Eighteenth Symposium (International) on Combustion, Waterloo, Ontario, August 1980. (c) Smith, G.P. and Crosley, D.R., "Energy Transfer in $A^2\Sigma^+$ OH in Flames," Paper FA9, Thirty-fifth Symposium on Molecular Spectroscopy, Columbus, Ohio, June 1980. (d) Smith, G.P. and Crosley, D.R., "Rotational Energy Transfer and LIF Temperature Measurements," submitted for publication.
5. (a) Anderson, W.R., "Laser Excited Fluorescence Measurement of OH Rotational Temperatures in a CH_4/N_2O Flame," Paper 3, Eastern Section Fall Meeting of the Combustion Institute, Atlanta, Georgia, Nov. 1979. (b) Anderson, W.R., Beyer, R.A. and Vanderhoff, J.A., "Laser Excited Fluorescence, Laser Raman and Band Reversal Temperature Measurements in CH_4/N_2O Flames," Paper FA1, Thirty fifth Symposium on Molecular Spectroscopy, Columbus, Ohio, June 1980.
6. Anderson, W.R., unpublished results.
7. DeWilde, M.A., "Capillary Flowmeters for Accurate, Stable Flows of Gases," BRL Technical Report No. ARBRL-TR-02230, 1980. (AD A083874)
8. Dieke, G.H. and Crosswhite, H.M., "The Ultraviolet Bands of OH," J. Quant. Spectrosc. Radiat. Transfer, Vol. 2, p. 97, 1962.
9. (a) Anderson, W.R., Decker, L.J. and Kotlar, A.J., "Measurement of OH and NH Concentration Profiles in Stoichiometric CH_4/N_2O Flames by Laser Excited Fluorescence," Paper 67, Eastern Section Fall Meeting of the Combustion Institute, Princeton, New Jersey, Nov. 1980. (b) Anderson, W.R., Kotlar, A.J. and Decker, L.J., "Concentration Profiles of OH and NH in a Stoichiometric CH_4/N_2O Flame by Laser Excited Fluorescence and Absorption," to appear in Combustion and Flame.
10. (a) Chidsey, I.L. and Crosley, D.R., "Calculated Rotational Transition Probabilities for the A-X System of OH," J. Quant. Spectrosc. Radiat. Transfer, Vol. 23, p. 187, 1980.

REFERENCES

Similar calculations have been performed by: (b) Dimpfl, W.L. and Kinsey, J.L., "Radiative Lifetimes of OH ($A^2\Sigma^+$) and Einstein Coefficients for the A-X System of OH and OD," J. Quant. Spectrosc. Radiat. Transfer, Vol. 21, p. 233, 1979. (c) Goldman, A. and Gillis, J.R., "Spectral Line Parameters for the $A^2\Sigma - X^2\Pi(0,0)$ Band of OH for Atmospheric and High Temperatures," submitted for publication.

11. Luck, K.C. and Muller, F.J., "Simultaneous Determination of Temperature and OH Concentration in Flames Using High Resolution Laser-Absorption Spectroscopy," J. Quant. Spectrosc. Radiat. Transfer, Vol. 17, p. 403, 1977.
12. Svehla, R.A. and McBride, B.J., Fortran IV Computer Program for Calculation of Thermodynamic and Transport Properties of Complex Chemical Systems," NASA TN D-7056, 1973.
13. Anderson, W.R., "Measurement of the Line Reversal Temperature of OH in CH_4/N_2O Flames," BRL Technical Report No. ARBRL-TR-02280, Jan. 1981. (AD A095349)
14. Beyer, R.A. and Vanderhoff, J.A., "Raman Spectroscopy of Premixed CH_4/N_2O Flames," BRL Report, to be published.
15. Snelleman, W., "Errors in the Method of Line-Reversal" Combustion and Flame, Vol. 11, p. 453, 1967 and Ref. 16.
16. Gaydon, A.G. and Wolfhard, H.G.W., "Flames: Their Structure, Radiation and Temperatures," Chapman and Hall, Ltd., London, 1970.
17. Crosley, D.R., private communication.
18. (a) Lengel, R.K. and Crosley, D.R., "Energy Transfer in $A^2\Sigma^+$ OH. II. Vibrational," J. Chem. Phys., Vol. 68, p. 5309, 1978. (b) Crosley, D.R. and Smith, G.P., "Vibrational Energy Transfer in $A^2\Sigma^+$ OH in Flames," Paper 69, Eastern Section Fall Meeting of the Combustion Institute, Princeton, New Jersey, Nov. 1980.
19. German, K.R. "Collision and Quenching Cross Sections in the $A^2\Sigma^+$ State of OH and OD," J. Chem. Phys., Vol. 64, p. 4065, 1976.
20. Sutherland, R.A. and Anderson, R.A., "Radiative and Predissociative Lifetimes of the $A^2\Sigma^+$ State of OH," J. Chem. Phys., Vol. 58, p. 1226, 1973.
21. Lucht, R.P. Sweeney, D.W. and Laurendeau, N.M., "Saturated Fluorescence Measurements of the Hydroxyl Radical," in Laser Probes for Combustion Chemistry, (D.R. Crosley, ed.), ACS Symposium Series 134, American Chemical Society, Washington, D.C., 1980, p. 145.

REFERENCES

22. Cattolica, R.J., "OH Rotational Temperature from Two-Line Laser Fluorescence," Appl. Opt., Vol. 20, p. 1156, 1981.

APPENDIX A

LINE-FITTING THEORY

APPENDIX A

LINE-FITTING THEORY

The fitting routine takes into account the laser lineshape, Doppler and collisional broadening, the number density, the temperature, parameters associated with the experimental design such as baselines and scaling factors for the fluorescence experiment, and absolute and relative frequency values for both the absorption and fluorescence data. For the simultaneous fitting of both absorption and fluorescence data the above set includes nineteen parameters. These are always chosen to be the minimum number of parameters necessary without fixing any parameter to a predetermined value which would introduce a bias into the fit.

The vibrational, rotational and translational temperatures are assumed to be the same. The analysis of the data utilizes a multi-parameter, nonlinear weighted least squares fitting routine which is discussed in detail elsewhere*. The procedure requires initial guesses for the parameters which are then varied to minimize the sum of the squares of the differences between the observed and calculated values. Upon convergence, the variance/covariance matrix is calculated from which the standard deviation of each parameter, as statistically determined from the fit, is obtained.

The spectrum is fitted using either absorption or fluorescence equations, described briefly below, as appropriate to the particular type of data. The equations are derived in full elsewhere*. For the absorption experiment using a broadband detector, the transmitted intensity of a laser line centered at ν_0 and traveling a distance ℓ through a flame is

$$I(\nu_0, \ell) = \int I_{\nu,0}(\nu_0) \exp \left\{ (-h\nu\ell/c) \left[\frac{N_T}{Q(T)} \sum_j B_j g_j \exp(-E_j/kT) P_j \right] \right\} d\nu. \quad (A1)$$

Here, h is Planck's constant, c is the speed of light, and the sum over j denotes the transitions (two to five) included in the fit. B_j is the absolute Einstein coefficient of absorption for the j th transition, in units appropriate to energy density, as given by Dimpfl and Kinsey^{10b}. g_j is the degeneracy of the j th sublevel and E_j its energy, k the Boltzmann constant and T the temperature. Finally, N_T is the total number density, $Q(T)$ is the partition function, P_j is the transition lineshape (Voigt profile)** and $I_{\nu,0}(\nu)$ is the incident frequency profile of the laser. A Gaussian function is chosen as the appropriate

* Kotlar, A.J. and Anderson, W.R., "A Method for the Determination of Temperature and Concentration of OH Using Fluorescence and Absorption Spectroscopy," BRL Report to be published.

** Armstrong, B.H., "Spectrum Line Profiles: The Voigt Function," J. Quant. Spectrosc. Radiat. Transfer, Vol. 7, p. 61, 1967.

representation of a multi-mode laser exhibiting amplitude fluctuations when averaged over several pulses***.

The fluorescence signal, F , is assumed to be proportional to the number of photons absorbed over a certain pathlength of the laser beam in the flame. The pathlength observed is between two limits, l_1 and l_2 , as defined by the collection optics and the monochromator slitwidth. F is thus given by

$$F = S [I(\nu_0, l_1) - I(\nu_0, l_2)] \quad (A2)$$

where S is a scaling factor which depends on the geometry of the experiment, the efficiency of quenching of excited molecules, redistribution of molecules into states other than the one originally excited by the laser, and the bandpass for the collection of fluorescence as defined by the detector. Note that this procedure automatically accounts for any small laser depletions.

$I(\nu_0, l)$ in Eq. [A1] was evaluated by numerical integration over ν . The limits of integration were chosen to include more than 99% of the laser profile. Evaluation of Eq. [A1] or [A2] for each datum (ν_0) then generates the absorption and fluorescence spectra which are fitted to the observed spectra using the least squares technique discussed previously.

*** Yuratic, M.A., "Effects of Laser Linewidth on Coherent Anti-Stokes Raman Spectroscopy," Molecular Physics, Vol. 38, p. 625, 1979.

DISTRIBUTION LIST

<u>No. of Copies</u>	<u>Organization</u>	<u>No. of Copies</u>	<u>Organization</u>
12	Administrator Defense Technical Info Center ATTN: DTIC-DDA Cameron Station Alexandria, VA 22314	1	Director US Army ARRADCOM Benet Weapons Lab ATTN: DRDAR-LCB-TL Watervliet, NY 12189
1	Director Defense Advanced Research Projects Agency ATTN: LTC C. Buck 1400 Wilson Boulevard Arlington, VA 22209	1	Commander US Army Watervliet Arsenal ATTN: Code SARWV-RD, R. Thierry Watervliet, NY 12189
2	Director Inst for Defense Analysis ATTN: H. Wolfhard R.T. Oliver 1801 Beauregard St. Alexandria, VA 22311	1	Commander US Army Aviation Research and Development Command ATTN: DRDAV-E 4300 Goodfellow Blvd St. Louis, MO 63120
1	Commander US Army Materiel Development and Readiness Command ATTN: DRCDMD-ST 5001 Eisenhower Avenue Alexandria, VA 22333	1	Director US Army Air Mobility Research and Development Laboratory Ames Research Center Moffett Field, CA 94035
2	Commander US Army Armament Research and Development Command ATTN: DRDAR-TSS Dover, NJ 07801	1	Commander US Army Communications Rsch and Development Command ATTN: DRDCO-PPA-SA Fort Monmouth, NJ 07703
5	Commander US Army Armament Research and Development Command ATTN: DRDAR-LCA, D. Downs DRDAR-LC, L. Harris DRDAR-SCA, L. Stiefel DRDAR-LCE, R.F. Walker DRDAR-TDC Dover, NJ 07801	1	Commander US Army Electronics Research and Development Command Technical Support Activity ATTN: DELSD-L Fort Monmouth, NJ 07703
1	Commander US Army Armament Materiel Readiness Command ATTN: DRSAR-LEP-L, Tech Lib Rock Island, IL 61299	1	Commander US Army Missile Command ATTN: DRSMI-R Redstone Arsenal, AL 35898
		1	Commander US Army Missile Command ATTN: DRSMI-YDL Redstone Arsenal, AL 35898

DISTRIBUTION LIST

<u>No. of Copies</u>	<u>Organization</u>	<u>No. of Copies</u>	<u>Organization</u>
1	Commander US Army Natick Research and Development Command ATTN: DRXRE, D. Sieling Natick, MA 01762	1	Commander Naval Sea Systems Command ATTN: J.W. Murrin, SEA-62R2 National Center Bldg. 2, Room 6E08 Washington, DC 20362
1	Commander US Army Tank Automotive Research & Development Gnd ATTN: DRDTA-UL Warren, MI 48090	1	Commander Naval Surface Weapons Center ATTN: Library Br., DX-21 Dahlgren, VA 22448
1	Commander US Army White Sands Missile Range ATTN: STEWS-VT White Sands, NM 88002	2	Commander Naval Surface Weapons Center ATTN: S.J. Jacobs/Code 240 Code 730 Silver Spring, MD 20910
1	Commander US Army Materials and Mechanics Research Center ATTN: DRXMR-ATL Watertown, MA 02172	1	Commander Naval Underwater Systems Gnd. Energy Conversion Department ATTN: R.S. Lazar/Code 5B331 Newport, RI 02840
5	Commander US Army Research Office ATTN: Tech Lib D. Squire F. Schmiedeshaff R. Ghirardelli M. Ciftan P. O. Box 12211 Research Triangle Park NC 27709	2	Commander Naval Weapons Center ATTN: R. Derr C. Thelen China Lake, CA 93555
		1	Commander Naval Research Laboratory ATTN: Code 6180 Washington, DC 20375
1	Director US Army TRADOC Systems Analysis Activity ATTN: ATAA-SL, Tech Lib White Sands Missile Range NM 88002	1	Commander Naval Research Laboratory Chem. Div. ATTN: J. McDonald Washington, DC 20375
2	Office of Naval Research ATTN: Code 473 G. Neece 800 N. Quincy Street Arlington, VA 22217	1	Sandia National Laboratories ATTN: D. Stephenson Div. 8351 Livermore, CA 94550

DISTRIBUTION LIST

<u>No. of Copies</u>	<u>Organization</u>	<u>No. of Copies</u>	<u>Organization</u>
3	Superintendent Naval Postgraduate School ATTN: Tech Lib D. Netzer A. Fuhs Monterey, CA 93940	1	Aerojet Solid Propulsion Co. ATTN: P. Michell Sacramento, CA 95813
		1	ARO Incorporated Arnold AFB, TN 37389
2	Commander Naval Ordnance Station ATTN: Dr. Charles Dale Tech Lib Indian Head, MD 20640	1	Atlantic Research Corporation ATTN: M.K. King 5390 Cherokee Avenue Alexandria, VA 22314
2	AFOSR ATTN: D. Ball L. Caveny Bolling AFB, DC 20332	1	AVCO Everett Research Lab Div ATTN: D. Stickler 2385 Revere Beach Parkway Everett, MA 02149
2	AFRPL (DYSC) ATTN: D. George J.N. Levine Edwards AFB, CA 93523	2	Calspan Corporation ATTN: E.B. Fisher A.P. Trippe P.O. Box 400 Buffalo, NY 14225
6	National Bureau of Standards ATTN: J. Hastie T. Kashiwagi H. Semerjian M. Jacox K. Smyth J. Stevenson Washington, DC 20234	2	Exxon Research & Engineering ATTN: A. Dean M. Chou P.O. Box 45 Linden, NJ 07036
1	General Motors Rsch Labs Physics Department ATTN: J.H. Bechtel Warren, Michigan 48090	1	Foster Miller Associates ATTN: A.J. Erickson 135 Second Avenue Waltham, MA 02154
1	Lockheed Missiles & Space Co. ATTN: Tech Info Ctr 3521 Hanover Street Palo Alto, CA 94304	1	General Electric Company Armament Department ATTN: M.J. Bulman Lakeside Avenue Burlington, VT 05402
1	System Research Labs ATTN: L. Goss 2600 Indian Ripple Rd Dayton, Ohio 45440	1	General Electric Company Flight Propulsion Division ATTN: Tech Lib Cincinnati, OH 45215

DISTRIBUTION LIST

<u>No. of Copies</u>	<u>Organization</u>	<u>No. of Copies</u>	<u>Organization</u>
1	General Electric Corp. R&D ATTN: M. Drake P.O. Box 8, Bldg, K1, Rm. 51326 Schenectady, N.Y. 12301	1	Pulsepower Systems, Inc. ATTN: L.C. Elmore 815 American Street San Carlos, CA 94070
2	Hercules Incorporated Allegheny Ballistic Lab ATTN: R. Miller Tech Lib P. O. Box 210 Cumberland, MD 21501	3	Rockwell International Corp. Rocketdyne Division ATTN: C. Obert J.E. Flanagan A. Axeworthy 6633 Canoga Avenue Canoga Park, CA 91304
1	Hercules Incorporated Bacchus Works ATTN: B. Isom Magna, UT 84044	1	Hercules, Inc. Industrial Systems Dept. P. O. Box 548 McGregor, TX 76657
1	IBM Corp ATTN: A.C. Tam Research Div. 5600 Cottle Rd San Jose, CA 95193	1	Science Applications, Inc ATTN: R.B. Edelman Combustion Dynamics & Propulsion Division 23146 Comorah Crest Woodland Hills, CA 91364
1	United Technologies ATTN: A. C. Eckbreth East Hartford, CT 06108	1	Shock Hydrodynamics, Inc ATTN: W.H. Anderson 4710-16 Vineland Avenue N. Hollywood, CA 91602
1	Olin Corporation Badger Army Ammunition Plant ATTN: J. Ramnarace Baraboo, WI 53913	1	Thiokol Corporation Elkton Division ATTN: E. Sutton Elkton, MD 21921
1	Olin Corporation New Haven Plant 275 Winchester Ave. New Haven, CT 06504	3	Thiokol Corporation Huntsville Division ATTN: D. Flanigan R. Glick Tech Lib Huntsville, AL 35807
1	Paul Gough Associates, Inc ATTN: P.S. Gough P.O. Box 1614 Portsmouth, NH 03801	2	Thiokol Corporation Wasatch Division ATTN: J. Peterson Tech Lib P.O. Box 524 Brigham City, UT 84302
1	Physics International Co 2700 Merced Street Leandro, CA 94577		

DISTRIBUTION LIST

<u>No. of Copies</u>	<u>Organization</u>	<u>No. of Copies</u>	<u>Organization</u>
1	TRW Systems Group ATTN: H. Korman One Space Park Redondo Beach, CA 90278	1	Institute of Gas Technology ATTN: D. Gidaspow 3424 S. State Street Chicago, IL 60616
2	United Technologies Chemical Systems Division ATTN: R. Brown Tech Lib P.O. Box 358 Sunnyvale, CA 94086	1	Johns Hopkins University/APL Chemical Propulsion Info Ag ATTN: T. Christian Johns Hopkins Road Laurel, MD 20810
3	Battelle Memorial Institute ATTN: Tech Lib 505 King Avenue Columbus, OH 43201	1	Massachusetts Inst. of Tech Dept of Mech Engineering ATTN: T. Toong Cambridge, MA 02139
2	Brigham Young University Dept of Chemical Engineering ATTN: M.W. Beckstead Provo, UT 84601	2	Pennsylvania State University Dept of Mechanical Eng ATTN: K. Kuo G. Faeth University Park, PA 16802
1	California Institute of Tech 204 Karmar Lab Mail Stop 301-46 ATTN: F.E.C. Culick 1201 E. California Street Pasadena, CA 91125	1	Pennsylvania State University Dept of Material Sciences ATTN: H. Palmer University Park, PA 16802
1	Case Western Reserve Univ Aerospace Sciences ATTN: J. Tien Cleveland, OH 44135	1	Polytechnic Institute of NY ATTN: S. Lederman Route 110 Farmingdale, NY 11735
1	Cornell University Department of Chemistry ATTN: E. Grant Baker Laboratory Ithaca, N.Y. 14853	1	Princeton Combustion Research Laboratories ATTN: M. Summerfield 1041 U.S. Highway One North Princeton, NJ 08540
3	Georgia Institute of Tech School of Aerospace Eng. ATTN: B.T. Zinn E. Price W.C. Strahle Atlanta, GA 30332	1	IITRI ATTN: M. J. Klein 10 West 35th Street Chicago, IL 60616
		3	Princeton University Forrestal Campus ATTN: I. Glassman K. Brezinsky Tech Lib P.O. Box 710 Princeton, NJ 08540

DISTRIBUTION LIST

<u>No. of Copies</u>	<u>Organization</u>	<u>No. of Copies</u>	<u>Organization</u>
4	Purdue University School of Mechanical Eng. ATTN: J. Osborn S.N.B. Murthy N.M. Laurendeau D. Sweeney TSPC Chaffee Hall W. Lafayette, IN 47906	1	University of California Dept. of Mechanical Eng. ATTN: J.W. Daily Berkeley, California 94720
1	Rensselaer Polytecnic Inst. Dept. of Chem. Engineering ATTN: A. Fontijn Troy, NY 12181	1	Univ. of Dayton University of Dayton Research Institute Dayton, OH 45406
1	Rutgers State University Dept of Mechanical and Aerospace Engineering ATTN: S. Temkin University Heights Campus New Brunswick, NJ 08903	1	University of Florida Dept. of Chemistry ATTN: J. Winefordner Gainesville, Florida 32601
1	Sandia Laboratories Combustion Sciences Dept. ATTN: R. Cattolica Livermore, CA 94550	1	University of Illinois Dept of Mechanical Eng. ATTN: H. Krier 144 MEB, 1206 W. Green St. Urbana, IL 61801
4	SRI International ATTN: Tech Lib D. Crosley J. Barker D. Golden 333 Ravenswood Avenue Menlo Park, CA 94025	1	University of Minnesota Dept of Mechanical Eng. ATTN: E. Fletcher Minneapolis, MN 55455
1	Stevens Institute of Tech Davidson Library ATTN: R. McAlevy, III Hoboken NJ 07030	2	University of California, Santa Barbara Quantum Institute ATTN: K. Schofield M. Steinberg Santa Barbara, CA 93106
1	University of California, San Diego Ames Department ATTN: F. Williams P.O. Box 109 La Jolla, CA 92037	1	University of Southern California Department of Chemistry ATTN: S. Benson Los Angeles, CA 90007
		1	Stanford University Department of Mech. Eng. ATTN: R. Hanson Stanford, CA 93106
		2	University of Texas Department of Chemistry ATTN: W. Gardiner H. Schaefer Austin, TX 78712

DISTRIBUTION LIST

<u>No. of Copies</u>	<u>Organization</u>
2	University of Utah Dept. of Chemical Engineering ATTN: A. Baer G. Flandro Salt Lake City, UT 84112

ABERDEEN PROVING GROUND

Dir, USAMSA
ATTN: DRXSY-D
DRXSY-MP, H. Cohen

Cdr, USATECOM
ATTN: DRSTE-TO-F

Dir, USACSL, Bldg E3516
ATTN: DRDAR-CLB-PA

USER EVALUATION OF REPORT

Please take a few minutes to answer the questions below; tear out this sheet, fold as indicated, staple or tape closed, and place in the mail. Your comments will provide us with information for improving future reports.

1. BRL Report Number _____

2. Does this report satisfy a need? (Comment on purpose, related project, or other area of interest for which report will be used.)

3. How, specifically, is the report being used? (Information source, design data or procedure, management procedure, source of ideas, etc.) _____

4. Has the information in this report led to any quantitative savings as far as man-hours/contract dollars saved, operating costs avoided, efficiencies achieved, etc.? If so, please elaborate.

5. General Comments (Indicate what you think should be changed to make this report and future reports of this type more responsive to your needs, more usable, improve readability, etc.) _____

6. If you would like to be contacted by the personnel who prepared this report to raise specific questions or discuss the topic, please fill in the following information.

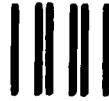
Name: _____

Telephone Number: _____

Organization Address: _____

FOLD HERE

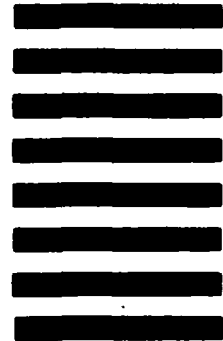
Director
US Army Ballistic Research Laboratory
Aberdeen Proving Ground, MD 21005



NO POSTAGE
NECESSARY
IF MAILED
IN THE
UNITED STATES

OFFICIAL BUSINESS
PENALTY FOR PRIVATE USE, \$300

BUSINESS REPLY MAIL
FIRST CLASS PERMIT NO 12062 WASHINGTON, DC
POSTAGE WILL BE PAID BY DEPARTMENT OF THE ARMY



Director
US Army Ballistic Research Laboratory
ATTN: DRDAR-TSB-S
Aberdeen Proving Ground, MD 21005

FOLD HERE

FILME
9